SJESR: Vol. 2, No.4, 2024, 78-94

IRAQI Academic Scientific Journals

SAMARRA JOURNAL OF ENGINEERING SCIENCE AND RESEARCH

S.J.E.S.R

Evaluating the Thermal Performance of Solar Water Heating System Used Polypropylene Glycol with Al_2O_3 Nanoparticles in Different Concentrations as a Thermal Medium

Rasha Yahya Al-Amiri [1]*, Ahmed Salih Al-Akaishi [2]

1- **Najaf Governorate Office, Reconstruction Authority, Najaf, Iraq**

2- **Mechanical Engineering Department, Faculty of Engineering, University of Kufa, Iraq**

Keywords

solar water heating system, polypropylene glycol, Al_2O_3 nanoparticles

Corresponding Author

Email: rashay.alameri@student.uokufa.edu.iq

Abstract

In this study, three laboratory samples of a nanofluid consisting of alumina in a propylene glycol solution were prepared for three different concentrations in weight ratios (0.2, 0.4, and 0.6%). The thermal conductivity and dynamic viscosity of the three concentrations were measured at different temperatures (20, 60, 100, 140, and 180) °C. The results showed that the concentration of 0.6% is the highest value for thermal conductivity, and it was chosen as a working fluid in the experimental device. The nanofluid was placed in copper tubes to act as a heat transfer fluid. Sunflower oil was used as a medium to store the heat acquired from solar radiation. The oil was placed inside the evacuated tube, and the spiral annular copper tube was immersed in the vegetable oil and the second copper tube inside the water tank. They were connected to each other with copper connectors and copper ball valves. The experimental device was operated on March 2, 2024, and the highest temperature of vegetable oil was recorded at 134.9 °C, nanofluid coming out of the water tank at 35.6 °C, nanofluid entering the water tank at 80 °C, and water temperature at 42 °C at 6 pm. The experimental device continued to operate, and on April 2, 2024, the highest temperatures of oil, outgoing liquid, incoming liquid, and water were recorded at (164.1, 62.9, 103, and 70.8) °C, respectively, at 6 pm. With the continued operation of the experimental device, there was a noticeable increase in temperatures, and the highest temperatures were recorded on May 15, 2024, for oil, outgoing liquid, incoming liquid, and water at (174.1, 69.4, 115.9, and 80) °C, respectively. At the same time, the intensity of solar radiation falling on the evacuated tube was calculated during the daytime hours from 8 am to 6 pm. The average solar radiation for one day was recorded and the amount of heat stored in sunflower oil and the amount of heat stored in water were calculated and the efficiency of the evacuated tube was calculated. The efficiency of the evacuated tube was (66%,54%,52%) For the days mentioned above.

1. Introduction

Solar collector technology has lately been a significant study topic due to the growing demand for renewable energy sources. Solar radiation is a pollution-free source of renewable energy. A solar collector is a device that collects solar energy from sunlight and turns it into thermal energy, which may subsequently be used to heat houses and businesses [1] Renewable energy is the best solution for the future of humanity. More energy is needed for the tremendous technological progress.

There are different types of solar collectors such as flat plate collectors, evacuated tube, parabolic trough and dish. Each type has its own working principles and efficiency. Although there are many economic problems facing the use of solar energy, increasing the efficiency of solar collectors helps reduce the cost of thermal energy absorbed by the collector. The thermal properties of the working fluid have been of great interest to researchers. Adding nanoparticles to the basic fluid is the key to increasing the efficiency of solar collectors. Some authors believe that there are many papers that discuss the effect of nanofluids on the solar collector [2, 3]. The thermal performance of an evacuated tube solar collector with magnetite/water nanofluid was investigated, and the photothermal efficiency of the evacuated tube solar collector was 72.8% [4].

The efficiency of a U-shaped tubular solar collector with an alumina/water nanofluid was experimentally determined. It was discovered that conductivity increases with concentration while decreasing with nanoparticle size [5]. An experimental study was carried out to explore the influence of alumina/distilled water nanofluid as a working fluid on the thermal efficiency of a fully evacuated tubular solar collector. The findings shown that nanofluids can be employed as working fluids in an evacuated tubular solar collector to absorb heat from solar radiation and efficiently transform solar energy into thermal energy [6]. Two identical evacuated tube solar water heaters were employed, one operating by thermosiphon (natural convection) and the other having 20 heat tubes charged with methanol as the working fluid at a 50% charge ratio [7].

Nano fluids can be employed as a traditional heat transfer fluid in solar energy systems, overcoming conventional fluids' limited thermal conductivity [8]. The effect of using nanofluid alumina/water as a working fluid on the energy efficiency and thermal energy of a flat solar collector was investigated. The study found that nanofluids boosted energy efficiency by 83.5% [9].

The performance of the flat solar collector was investigated with nanofluids. The findings revealed that raising the proportion of alumina fluid enhances thermal efficiency while decreasing the pressure [10]. There are two types of solar collectors: flat collectors and evacuated tube collectors. Because of the vacuum inside the tube, evacuated tube collectors are more efficient in low thermal insulation conditions [11]. One of the major benefits of employing low temperature systems (solar collectors) is that they are relatively simple and inexpensive. In addition, several working fluids are appropriate for use at low temperatures [12, 13].

Some researchers have used propylene glycol, but at different concentrations than this research and with different oxides such as titanium oxide, zinc oxide, and copper oxide, with different systems. Highly conductive nanoparticles placed in traditional fluids like distilled water, oil, and ethylene glycol can improve the thermal properties of the working fluid [14, 15].

This research aims to design the water solar heating system and improve the thermal performance of propylene glycol by adding Al_2O_3 nanoparticles in this system.

2. Experimental Work:

2.1 Preparing nanofluid

The base fluid propylene glycol was mixed with nanomaterials Al_2O_3 using magnetic stirrer for 20 min for three concentrations (0.2%, 0.4%, 0.6%). The samples were mixed in the magnetic mixing and stirring device shown in Figure 1 for 20 minutes for three concentrations of alumina nanoparticles powder with a propylene glycol solution. Then the suspended particles were dispersed using an ultrasonic device as in Figure 2 for 15 minutes to obtain complete homogeneity. The testing was carried out in the laboratory under stable atmospheric conditions. The purpose was to obtain the results of the properties of both thermal conductivity (k) and viscosity (μ) at temperatures ranging from 20°C to 180°C. The samples were placed on a convection heater, respectively.

The temperature of the nanofluid is measured over time using a thermometer, as shown in Figure 3. When the desired temperature is reached, readings are taken for the sample. The thermal conductivity reading is taken by the thermal sensor via a sensor placed in the nanofluid as in Figure 4, and then the viscosity is measured at the same temperature. The nanofluid were prepared and tested in labrotrary in the Nanotechnology Unit Laboratory, College of Engineering, University of Kufa. Using a viscosity device, shown in Figure 5, five readings were taken over a period of 60 days. The period between one reading and the next reading was 15 days.

Fig. 1. *Magnetic stirrer*

Fig. 2. *Ultrasound device*

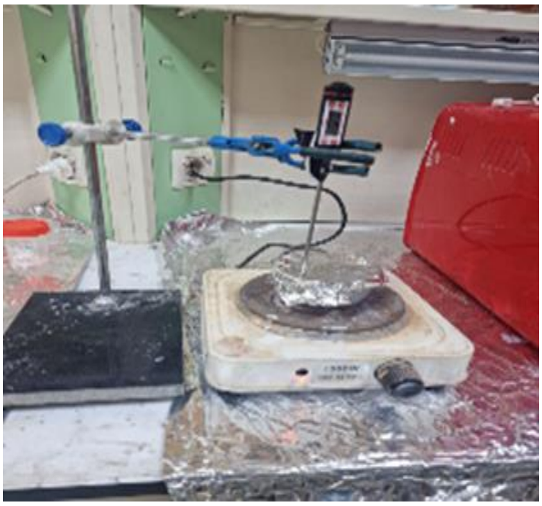

Fig. 3. *Thermal heater with thermometer*

Fig. 4. *Thermal conductivity measuring device*

Fig. 5. *Viscometer device*

The minimum value of thermal conductivity and viscosity was recorded in the first day test at 180 °C with (k = 0.13 W/m.K and μ = 13.2 cP). However, the addition of nanoparticles reversed the effect of temperature on the thermal conductivity of the resulting nanofluids. While k reached its maximum value (0.307 W/mK) at 180 °C for the nanofluid with 0.6% concentration on day (60) recording an improvement of (136.14%). In contrast, the viscosity continued to decrease with increasing temperature for each nanoparticle concentration. However, the concentration of nanoparticles is directly proportional to the dynamic viscosity at a constant temperature. In this competition, in the day (60) test, the viscosity at 20 °C for both pure PG and 0.6% Nano-PG was 58 and 64 cP, respectively. While at 180 °C, μ = 14.9 and 21 cP, respectively. The dynamic viscosity behavior of PG nanofluid at different concentrations and different temperatures has almost the same response to concentration and temperature as ethylene glycol-based nanofluid.

The evacuated tube used in this work is 1800 mm long, 58 mm outer diameter and 47 mm inner diameter as shown in figure 6. It was placed in an inclined direction at an angle depending on the geographical location, where it receives sunlight throughout the day. Copper tube consists of 91.7% copper, 6.3% phosphorus and 2% silver. The copper tube spiral coil shown in the figure 7 inserted inside evacuated tube.

The melting rate is from 645 to 815 °C and the elongation rate is 7%. Copper is a highly conductive metal and has excellent thermal and electrical conductivity. It is a flexible metal and can be shaped to the desired shape. It can be easily shaped without breaking. It is also corrosion resistant, which makes it a durable metal for many applications. It is light in weight and is widely used in the manufacture of heat exchange equipment. It can withstand high pressure and high temperatures. This feature allows it to transfer hot liquids and gases with minimal heat loss.

Fig. 6. *The evacuated glass tube*

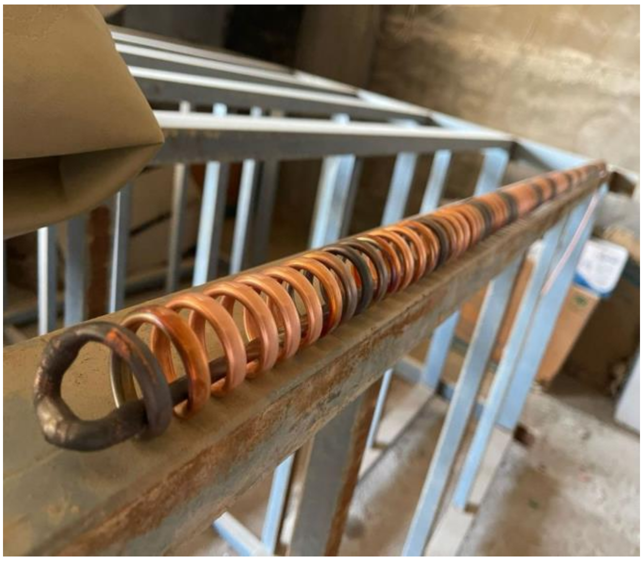

Fig. 7. *Copper tube spiral coil*

The water tank contains a copper tube that was hand-made from 24 pieces of copper tubes, each 18 cm long as shown in Figure 8. The ends of each tube are connected with a copper ring with a radius of 12 cm. Thus, the total length of the tube became 720 cm. The tank was filled with distilled water.

Fig. 8. *Copper tube installed inside the tank*

2.2 The Water Solar Heated System Procedures

1. Preparing and installing the evacuated tube on the mounting bracket base.

2. The mounting bracket base is installed facing south at an angle of 30 degrees from ground level.

3. Placing the spiral annular tube inside the evacuated tube.

4. The second copper tube was placed inside the water tank, fixed and connected to the ring tube by copper fittings.

5. Placing copper ball valves in the area where the two copper pipes connect.

6. A one-liter expansion tank was placed to which a nanofluid pressure measuring cage was attached inside the tubes.

7. Placing thermocouples in different places to measure the desired temperatures.

8. Sunflower oil was placed inside the evacuated tube as a medium to store the heat gained from the solar radiation falling on the tube.

9. The copper tubes were filled with the nanofluid through the expansion tank nozzle as shown in the figure 9.

10. The 45-liter water tank was filled with distilled water and lined with an insulating material to maintain the water temperature.

11. The intensity of solar radiation was measured for several days of the year (March, April, May, June, July and August) as shown in the figure 10.

Fig. 9. *Filling tubes with nanofluid*

Fig. 10. *Solar radiation meter*

3. Results and Discussion

3.1 Thermal Conductivity and Viscosity Results

The thermal conductivity was tested to determine which concentrations have the highest thermal conductivity and suitable viscosity at different temperatures starting from 20 to 180 °C. The results showed that the concentration of 0.6% is the highest conductivity as shown in the figure 11. The thermal conductivity of pure propylene glycol was measured over different time periods ranging from one day to 60 days with 15-day intervals between each test. It was found that the thermal conductivity increases with time since the beginning of preparation. Therefore, it is believed that the alumina nanoparticles interact more with propylene glycol, causing an increase in the thermal conductivity, as shown in Figure 12.

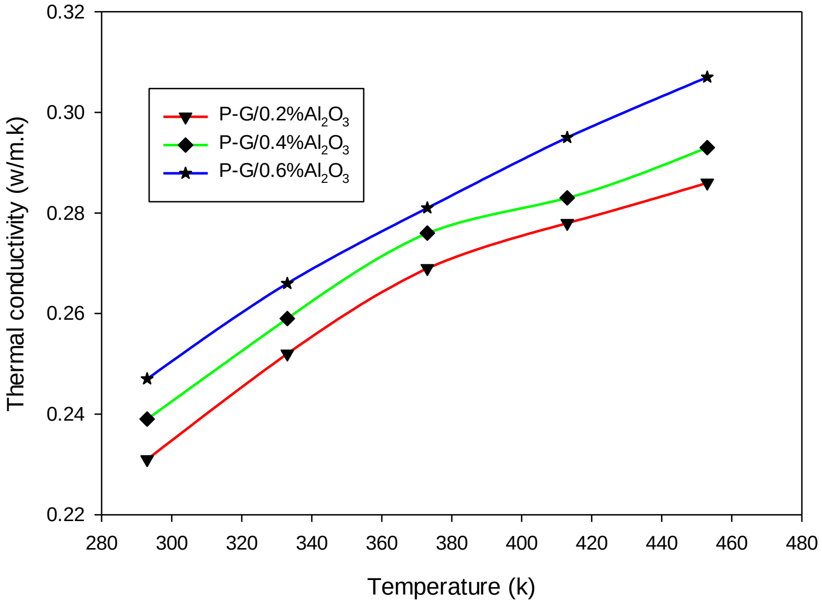

Fig. 11. *Relationship between temperature and thermal conductivity of propylene glycol with different concentrations of Al_2O_3 at (60 day)*

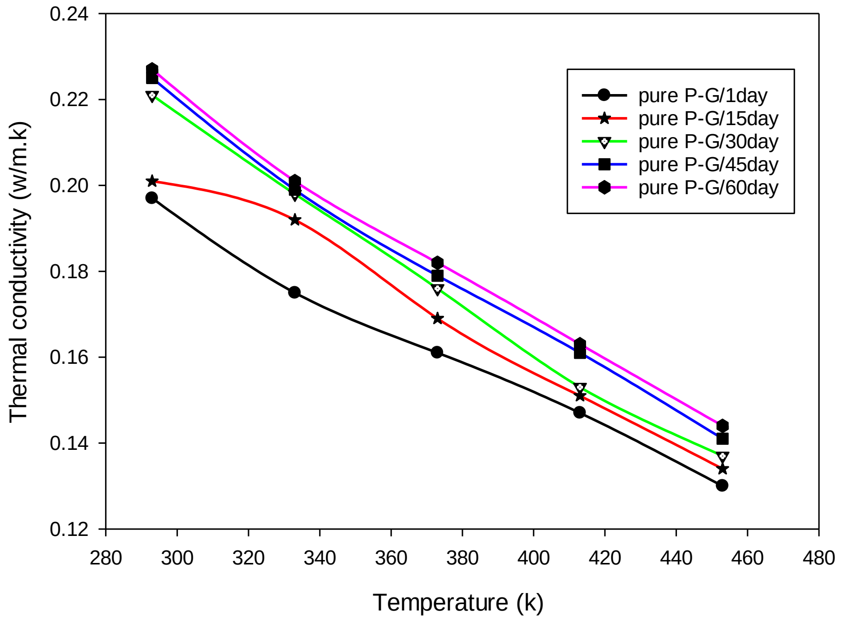

Fig. 12. *The relationship between temperature and thermal conductivity of pure propylene glycol liquid at different time periods*

Figures 13 and 14 show the three concentrations of nanofluids with different weight ratios of alumina nanoparticles (50-90 nm) in propylene glycol solution were prepared. It was observed that the viscosity of PG nanofluid increased with increasing nanoparticle concentration and decreased with increasing temperature. On the other hand, the pure liquid in terms of viscosity has the same response to temperature, it decreases with increasing temperature. However, the decrease in viscosity of pure PG nanofluid was slightly higher than that of PG nanofluid with respect to temperature. The highest recorded viscosity value (64 cp) at (20 °C) was for PG nanofluid at (0.6%) concentration on day (60) after the nanofluid preparation process. While the lowest recorded viscosity in these sets of experiments (13.2 cp) at (180 °C) was for pure PG in the first day tests. On day (60) of the tests, the viscosity was at the highest value among most of the other days tests. For example, at 20 °C, the viscosity of pure PG was 58 cP, while that of 0.6% PG nanofluid was 64 cP. Moreover, at the highest temperature (180 °C), the viscosity of pure PG was 14.9 cP, which was 74.31% lower than that at 20 °C. For 0.6% PG nanofluid, the viscosity was 21 cP, which was 67.19% lower than that at 20 °C. Here, the lower the viscosity of the nanofluid, the lower the pumping force required to circulate the nanofluid in solar thermal systems.

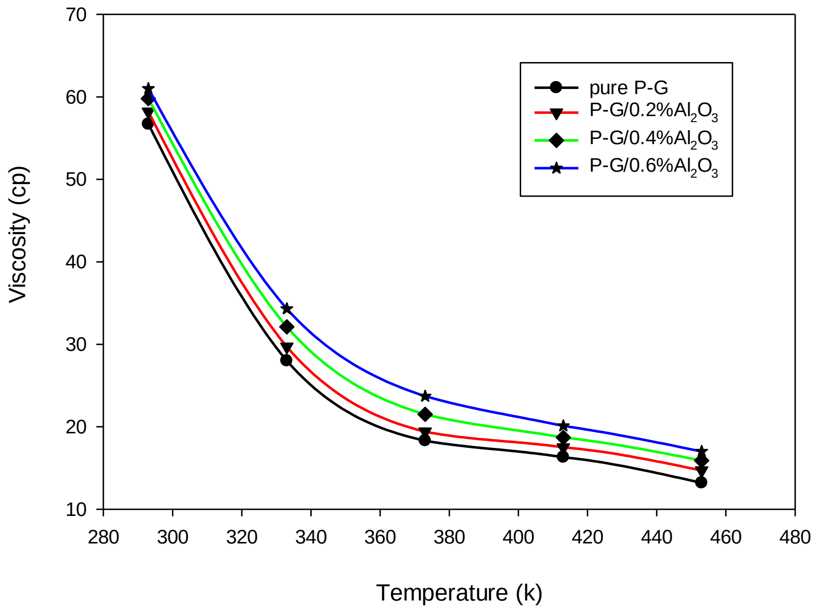

Fig. 13. *Relationship between temperature and viscosity of propylene glycol with different concentrations of Al_2O_3 at (1 day)*

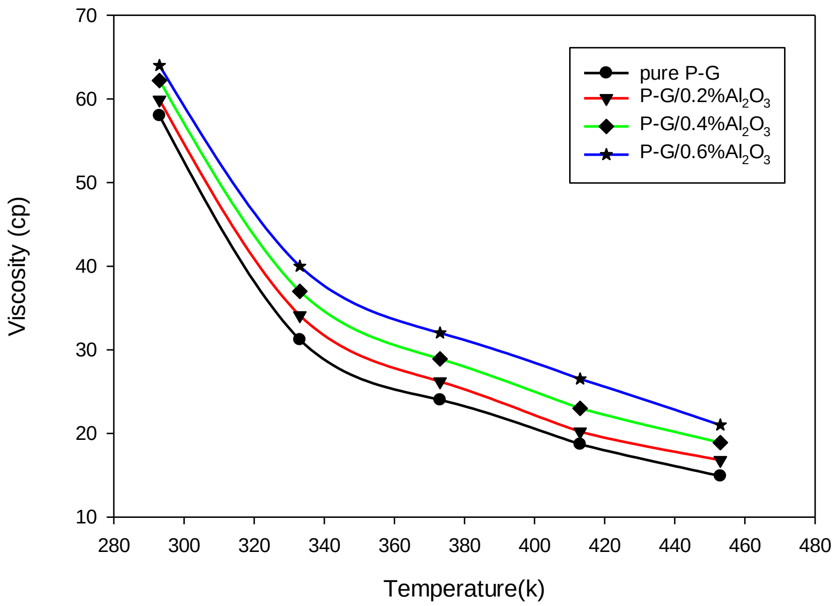

Fig. 14. *Relationship between temperature and viscosity of propylene glycol with different concentrations of Al_2O_3 at (60 day)*

3.2 Effect of Time Intervals on Temperatures

On March 2, 2024, the experimental device was turned on. Figure (15) shows the temperatures of the oil and nanofluid entering the water heater and the nanofluid exiting the water heater after heat exchange as well as the water temperature. The highest oil temperature was recorded at 134.9 °C, the water temperature was 42 °C, the temperature of the incoming nanofluid was 80 °C, and the temperature of the outgoing nanofluid was 35.6 °C at 6 pm. Physically, when the temperature of a pure liquid increases, the molecules of the liquid will move away from each other causing the liquid to expand. In this case, the heat transfer between the molecules will decrease due to the increasing gap between them. This widening of the gap also affects the thermal conductivity of the liquid inversely, such that the thermal conductivity of liquids decreases with increasing temperature. However, adding nanoparticles to a pure liquid under certain conditions is a game changer. The motion of the nanoparticles in the resulting nanofluid is governed by the theory of Brownian motion. According to this theory, the nanoparticles move and collide across the molecules of the liquid. The continuous collision between the solid nanoparticles enhances the heat transfer from one solid to another which in turn increases the overall thermal conductivity of the nanofluid. Brownian motion can be considered as a diffusion process with a diffusion coefficient (D) [16].

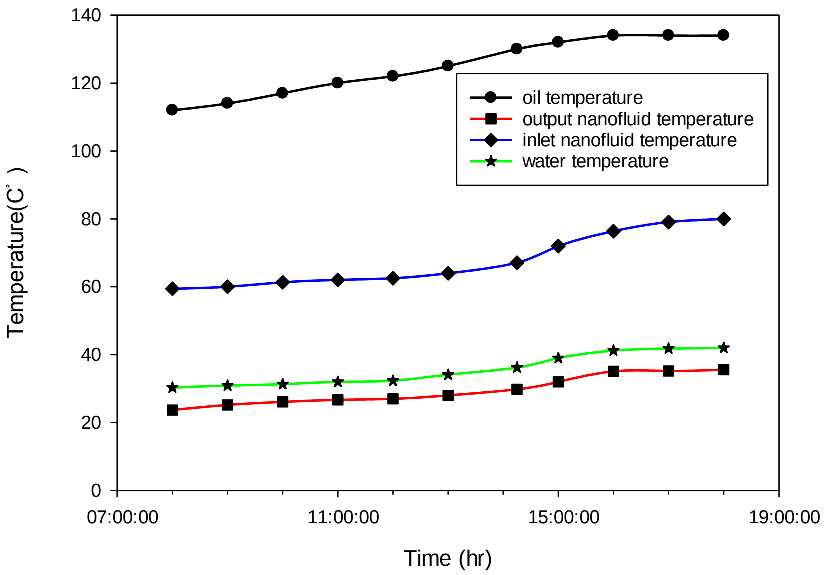

Fig. 15. *Relationship between temperature in degrees Celsius and time in hours*

On April 2, 2024, the experimental device continued to operate. Figure 16 shows the temperatures of the oil and the nanofluid entering the water heater and the nanofluid exiting the water heater after heat exchange and the water temperature. The highest oil temperature was recorded at 164.1 °C, the water temperature was 70.8 °C, the temperature of the incoming nanofluid was 103 °C, and the temperature of the outgoing nanofluid was 62.9 °C at 6 pm. The mechanism of the experimental device evacuated tube solar heater (ETST) is the flow of a nanofluid (aluminum oxide particles in a propylene glycol solution) inside copper tubes equipped in the form of a spiral tube to increase the heat exchange area. The first copper tube is immersed in sunflower oil inside the evacuated tube as shown above, and the second copper tube is immersed in the water tank, where the nanofluid acquires heat from the oil. The liquid flows inside the tube upwards to transfer heat to the water, where it works as a heat exchanger. The process is repeated throughout the day due to the presence of sunlight. Figure (15-16-17) shows the temperatures of each of the nanofluid inside the tubes, the oil temperature, and the water temperature over the days.

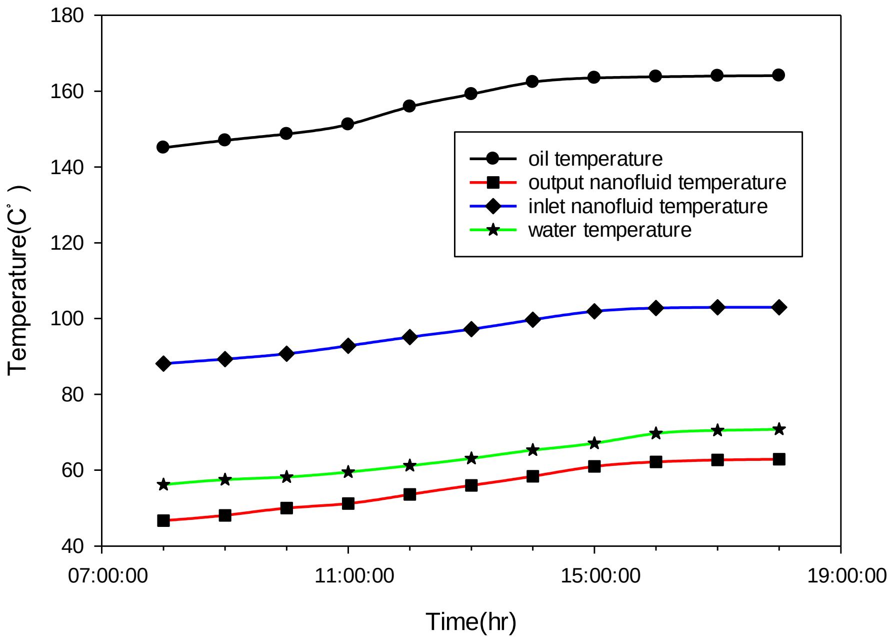

Fig. 16. *Relationship between temperature in degrees Celsius and time in hours*

On May 15, 2024, the experimental device continued to operate. Figure 17 shows the temperatures of the oil and the nanofluid entering the water heater and the nanofluid exiting the water heater after heat exchange and the water temperature. The highest oil temperature was recorded at 174.1 °C, the water temperature was 80 °C, the temperature of the incoming nanofluid was 115.9 °C, and the temperature of the outgoing nanofluid was 69.4 °C at 6 pm.

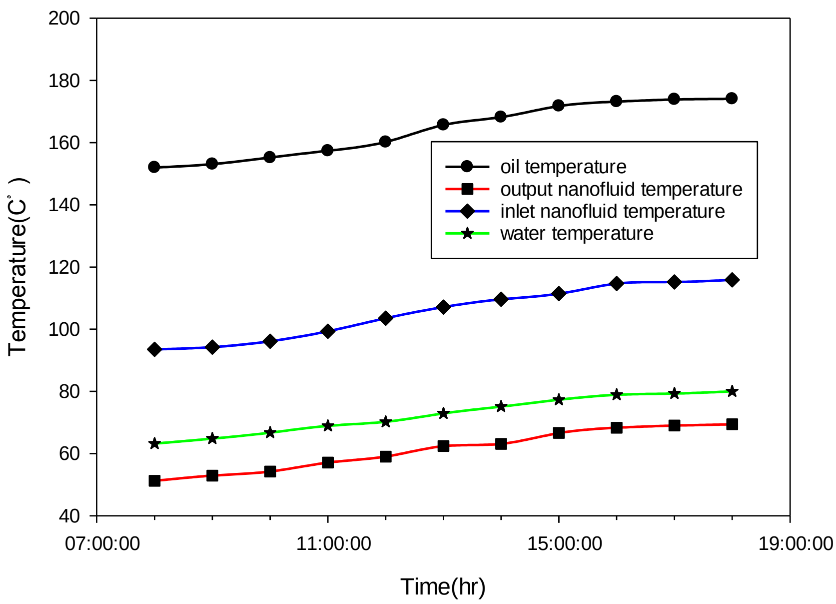

Fig. 17. *Relationship between temperature in degrees Celsius and time in hours*

3.3 Calculating stored energy and efficiency

To calculate the amount of thermal energy stored in the evacuated tube, the amount of heat acquired by the water, the amount of heat stored in the nanofluid, and to find the thermal efficiency, the following equations were applied [17];

$$\boldsymbol{Q = mc_p \, \Delta T} \qquad \textbf{(1)}$$

Q= Amount of energy stored per unit volume (W)

m= Mass of matter (Kg)

c_p = Specific heat capacity of a substance (KJ/Kg.K)

ΔT = Change in temperature (K)

$$\boldsymbol{\zeta = \frac{m\, c_p \ \Delta T}{I\, A_p}} \qquad \textbf{(2)}$$

$$\boldsymbol{Q_{abs=I_b A_p\, F_t}\ (\alpha\, \tau)} \qquad \textbf{(3)}$$

$Qabs$= Amount of energy absorbed (W)

I_b= Total solar radiation incident on the evacuated tube(W/m^2)

A_p = Surface area of evacuated tube (m^2)

F_t = Total coefficient of the effect of shade and dust on the amount of solar radiation

α = Glass cover permeability

τ = Absorbency of the absorption tube

α= 0.97, $\tau = 0.95$ ، $F_t = 0.9506$

The specific heat capacity of sunflower oil is equal to (2.244 KJ/Kg.K) [18]

1Sun (1000w/m^2) = 122000 Lux [19]

Calculating the amount of solar radiation is in watts/square meter.

Table 1. Solar radiation intensity rate for period from 2. March to 15. May

Today's date	Solar radiation intensity rate (Lux)	Solar radiation intensity rate (w/m^2)	Solar Evacuated Tube Energy (KJ)	Evacuated tube efficiency (%)
2/3/2024	80764	662	1942.38	66%
2/4/2024	87927	720.72	2115.036	54%
15/5/2024	99218	813.27	2386.65	52%

The absorbed energy depends on the solar radiation values. The more the solar radiation values increase, the more the absorbed energy values increase. It begins to increase gradually until it reaches its maximum value at the highest value of solar radiation intensity, after which it decreases. The thermal efficiency values depend on the stored energy values that are directly proportional to them. The more these values increase, the more the thermal efficiency values increase. In contrast, the absorbed energy values are inversely proportional to the thermal efficiency values. The more the absorbed energy values increase, which depend entirely on the solar radiation intensity values, the lower the thermal efficiency values. This is shown in equation (2).

3.3.1. Heat energy stored in oil

On March 2, 2024, the temperatures gained in the oil were recorded during the daytime hours from 8 am to 6 pm, where the energy gained was calculated in units (KJ) from the equation mentioned above, which is the product of multiplying the mass of the oil by the specific heat capacity of the oil by the change in temperature between one hour and the second that follows. The highest energy gained was recorded at 1 pm and the lowest energy at 4 pm. This difference is due to the change in temperature between one hour and the other, as the peak time is at 1 pm as shown in figure 18.

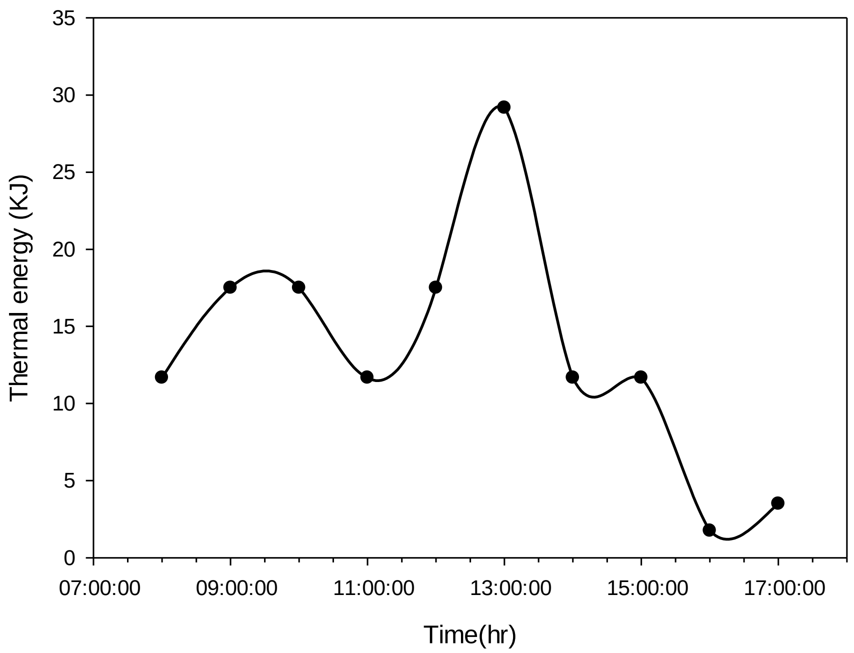

Fig. 18. *The relationship between the energy stored in oil (KJ) over time (hr)*

On April 2, 2024, the temperatures gained in the oil were recorded during the daytime hours from 8 am to 6 pm, where the energy gained was calculated in (KJ) from the equation mentioned above, which is the product of multiplying the mass of the oil by the specific heat capacity of the oil by the change in temperature between one hour and the second that follows. The highest energy gained was recorded at 11am and the lowest energy at 5 pm. This difference is due to the change in temperature between one hour and the other, as the peak time is at 11am as shown in figure 19.

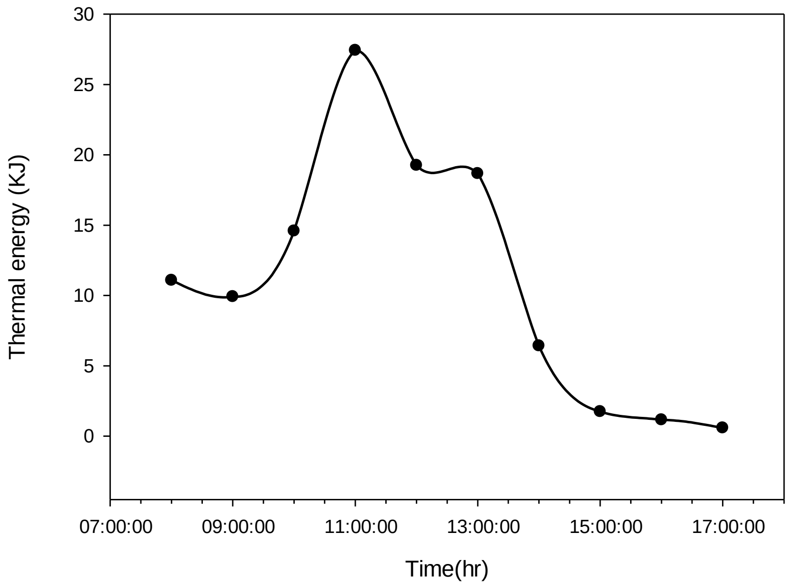

Fig. 19. *The relationship between the energy stored in oil (KJ) over time (hr)*

On May 15, 2024, the temperatures gained in the oil were recorded during the daytime hours from 8 am to 6 pm, where the energy gained was calculated in units (KJ) from the equation mentioned above, which is the product of multiplying the mass of the oil by the specific heat capacity of the oil by the change in temperature between one hour and the next. The highest energy gained was recorded at 12 pm and the lowest energy at 5 pm. This difference is due to the change in temperature between one hour and the next, as the peak time is at 12 pm as shown in figure 20.

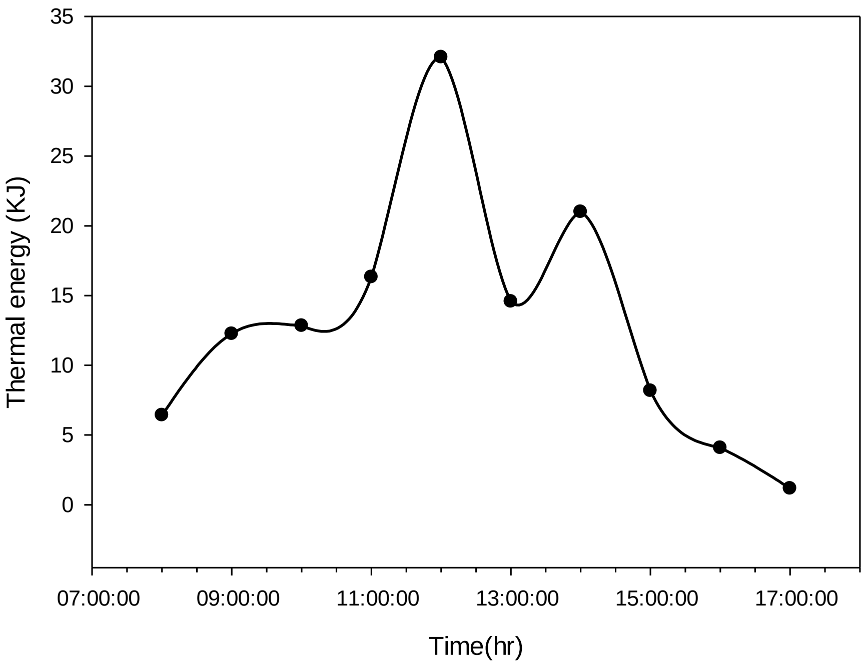

Fig. 20. *The relationship between the energy stored in oil (KJ) over time (hr)*

On March 2, 2024, the temperatures gained in water during the daytime hours from 8 am to 6 pm were recorded, where the energy gained was calculated in units (kilojoules) from the equation mentioned above, which is the product of the mass of water multiplied by the specific heat capacity of water with the change in temperature from one hour to another. The highest energy gained was recorded at 2 pm and the lowest energy at 5 pm. This difference is due to the change in temperature from one hour to another, as the peak time is at 2 pm as shown in figure 21.

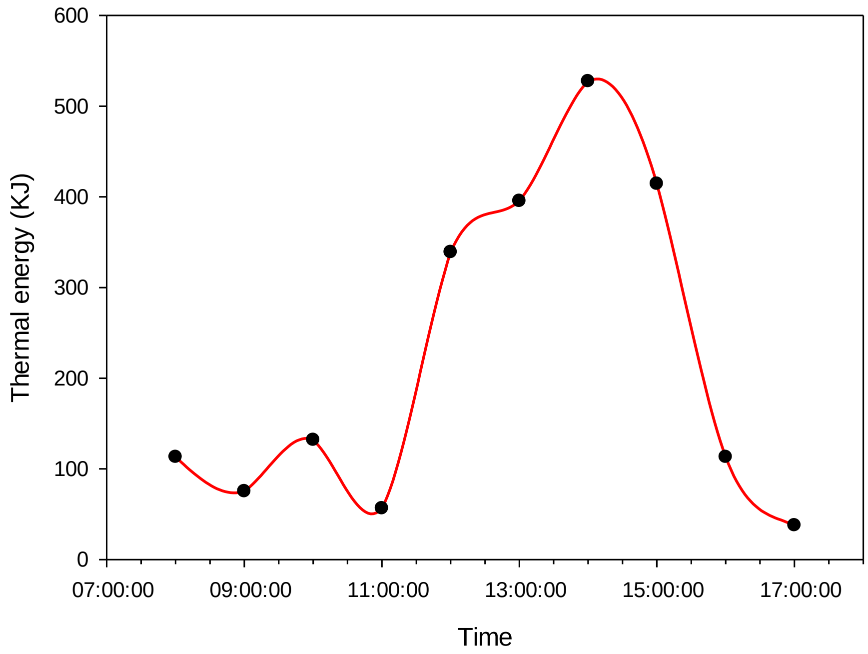

Fig. 21. *The relationship between the amount of energy stored in water (KJ) over time(hr)*

On April 2, 2024, the temperatures gained in water during the daytime hours from 8 am to 6 pm were recorded, where the energy gained was calculated in units (kilojoules) from the equation mentioned above, which is the product of the mass of water and the specific heat capacity of water with the change in temperature from one hour to another. The highest energy gained was recorded at 3 pm and the lowest energy at 5 pm. This difference is due to the change in temperature from one hour to another, as the peak time is at 3 pm as shown in figure 22.

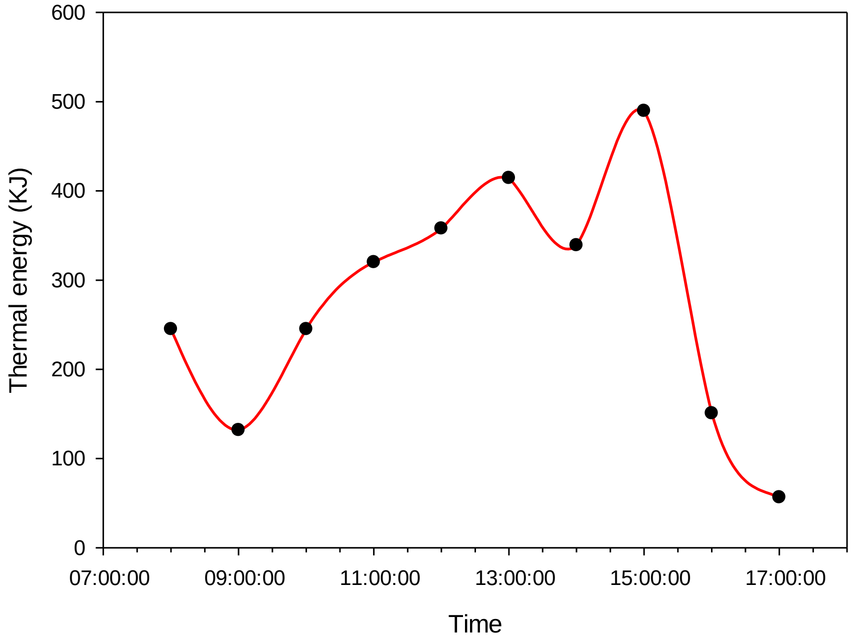

Fig. 22. *The relationship between the amounts of energy stored in water (KJ) over time (hr)*

On May 15, 2024, the temperatures gained in water during the daytime hours from 8 am to 6 pm were recorded, where the energy gained was calculated in units (kilojoules) from the equation mentioned above, which is the product of the mass of water and the specific heat capacity of water with the change in temperature from one hour to another. The highest energy gained was recorded at 12 noon and the lowest energy at 4 pm. This difference is due to the change in temperature from one hour to another, as the peak time is at 12 pm as shown in figure 23.

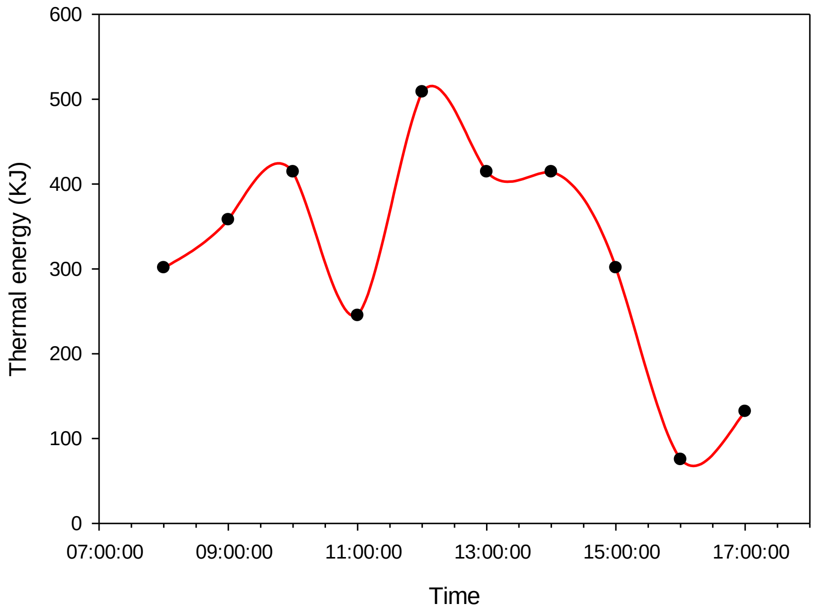

Fig. 23. *The relationship between the amount of energy stored in water (KJ) over time(hr)*

4. Conclusions

The properties of the propylene glycol-based nanofluids were measured over a temperature range of 20°C to 180°C using laboratory tests. The results showed that the concentration of 0.6% had the highest thermal conductivity value and was chosen as the working fluid in the experimental apparatus. The nanofluid was placed in copper tubes to act as a heat transfer fluid. Sunflower oil was used as a medium to store the heat gained from solar radiation. The oil was placed inside the evacuated tube. The spiral copper tube was immersed in the vegetable oil and the second copper tube was inside the water tank. They were connected with copper connectors and copper ball valves. The experimental device was operated on March 2, 2024, and the highest temperatures were recorded for vegetable oil at 134.9 °C, for the nanofluid coming out of the water tank at 35.6 °C, and for the nanofluid entering the water tank at 80 °C. The water temperature was 42 °C at 6 pm. The average solar radiation (662 w/m^2) and the amount of energy absorbed by the evacuated tube (1942.38 KJ) and the efficiency of the evacuated tube (66%) were recorded. The experimental device continued to operate, and the highest temperatures for the oil, the liquid coming out, the liquid coming in, and the water were recorded on April 2, 2024 at (164.1, 62.9, 103, and 70.8) °C, respectively, at 6 pm. The average solar radiation (720.72 w/m^2) and the amount of energy absorbed by the evacuated tube (2115.036 KJ) and the efficiency of the tube (54%) were recorded. With the continued operation of the experimental device, there are A significant rise in temperatures, as temperatures were recorded on May 15, 2024. The highest temperature of oil, external and internal fluid and water (174.1, 69.4, 115.9 and 80) °C, respectively, at 6 pm, where the average solar radiation (813.27 w/m^2) and the amount of energy absorbed by the evacuated tube (2386.65 KJ) and the tube efficiency (52%) were recorded. The intensity of solar radiation falling on the evacuated tube was calculated for daylight hours from 8 am to 6 pm.

Acknowledgements

The authors would like to acknowledge the assistance offered the staff of the Nanotechnology and Advanced Materials Research Unit.

References

1. SON, H. S., KWON, J. W., LEE, S. H., KIM, C., & HONG, H. (2014). The effect of upper-heating system in solar water storage tank. International Journal of Air-Conditioning and Refrigeration, 22(04), 1450027.
2. Samir Sami Abed, Mehdi Sedighi and Abbas Ali Diwan, (2023). Influence of Al_2O_3 Nano Additives on the Viscosity and Thermal Conductivity of Double Distilled Water. Kufa Journal of Engineering Vol. 14, No.2, 2023, (12-23).
3. Hussein, A. K. (2016). Applications of nanotechnology to improve the performance of solar collectors–Recent advances and overview. Renewable and Sustainable Energy Reviews, 62, 767-792.
4. Verma, S. K., & Tiwari, A. K. (2015). Progress of nanofluid application in solar collectors: a review. Energy Conversion and Management, 100, 324-346.
5. Sharafeldin, M. A., & Gróf, G. (2019). Efficiency of evacuated tube solar collector using WO3/Water nanofluid. Renewable energy, 134, 453-460.
6. Kim, H., Kim, J., & Cho, H. (2017). Experimental study on performance improvement of U-tube solar collector depending on nanoparticle size and concentration of Al2O3 nanofluid. Energy, 118, 1304-1312.

7. Ghaderian, J., & Sidik, N. A. C. (2017). An experimental investigation on the effect of Al2O3/distilled water nanofluid on the energy efficiency of evacuated tube solar collector. International Journal of heat and mass transfer, 108, 972-987.
8. Al-Joboory, H. N. S. (2019). Comparative experimental investigation of two evacuated tube solar water heaters of different configurations for domestic application of Baghdad-Iraq. Energy and Buildings, 203, 109437.
9. Said, Z., Iqbal, M., Mehmood, A., Le, T. T., Ali, H. M., Cao, D. N., ... & Pham, N. D. K. (2023). Nanofluids-based solar collectors as sustainable energy technology towards net-zero goal: Recent advances, environmental impact, challenges, and perspectives. Chemical Engineering and Processing-Process Intensification, 109477.
10. Said, Z., Saidur, R., Sabiha, M. A., Hepbasli, A., & Rahim, N. A. (2016). Energy and exergy efficiency of a flat plate solar collector using pH treated Al2O3 nanofluid. Journal of Cleaner Production, 112, 3915-3926.
11. Hawwash, A. A., Rahman, A. K. A., Nada, S. A., & Ookawara, S. (2018). Numerical investigation and experimental verification of performance enhancement of flat plate solar collector using nanofluids. Applied Thermal Engineering, 130, 363-374.
12. Naghavi, M. S., Ong, K. S., Mehrali, M., Badruddin, I. A., & Metselaar, H. S. C. (2015). A state-of-the-art review on hybrid heat pipe latent heat storage systems. Energy Conversion and Management, 105, 1178-1204.
13. Mehrali, M., Sadeghinezhad, E., Azizian, R., Akhiani, A. R., Latibari, S. T., Mehrali, M., & Metselaar, H. S. C. (2016). Effect of nitrogen-doped graphene nanofluid on the thermal performance of the grooved copper heat pipe. Energy Conversion and Management, 118, 459-473.
14. Alipour, H., Karimipour, A., Safaei, M. R., Semiromi, D. T., & Akbari, O. A. (2017). Influence of T-semi attached rib on turbulent flow and heat transfer parameters of a silver-water nanofluid with different volume fractions in a three-dimensional trapezoidal microchannel. Physica E: Low-Dimensional Systems and Nanostructures, 88, 60-76.
15. Colangelo, G., Favale, E., Miglietta, P., de Risi, A., Milanese, M., & Laforgia, D. (2015). Experimental test of an innovative high concentration nanofluid solar collector. Applied Energy, 154, 874-881.
16. Sadeghinezhad, E., Mehrali, M., Saidur, R., Mehrali, M., Latibari, S. T., Akhiani, A. R., & Metselaar, H. S. C. (2016). A comprehensive review on graphene nanofluids: Recent research, development and applications. Energy Conversion and Management, 111, 466-487.
17. Mukherjee, S., Mishra, P.C., Parashar, S.K.S. et al. (2016) Role of temperature on thermal conductivity of nanofluids: a brief literature review. Heat Mass Transfer 52, 2575–2585.
18. Daghigh, R., & Shafieian, A. (2016). Theoretical and experimental analysis of thermal performance of a solar water heating system with evacuated tube heat pipe collector. Applied Thermal Engineering, 103, 1219-1227.
19. Fasina, O. O., & Colley, Z. (2008). Viscosity and specific heat of vegetable oils as a function of temperature: 35 C to 180 C. International journal of food properties, 11(4), 738-746.